BENCHMARK TESTS FOR THE ESTIMATION OF POWER SPECTRA FROM LDA SIGNALS

L. H. Benedict
Lehrstuhl für Strömungsmechanik, University of Erlangen-Nürnberg
Cauerstr. 4, 91058 Erlangen, Germany

H. Nobach
Dantec Measurement Technology
Tonsbakken 16-18, 2740 Skovlunde, Denmark

C. Tropea
FG Strömungslehre und Aerodynamik (SLA), Technische Universität Darmstadt
Petersenstr. 30, 64287 Darmstadt, Germany

ABSTRACT

A set of 34 simulated data sets for the testing of power spectrum algorithms for LDA data has been created and made available at the internet address http://www-nt.e-technik.uni-rostock.de/~nobach/benchm.html. In this paper the characteristics and diagnostic intent of the data sets are described, as are initial results from 7 research groups who have tested 10 algorithms using these data sets. The results have highlighted strengths and weaknesses of the algorithms as well as the test cases. The initial results indicate that two modified versions of the slotting technique, a refinement for sample-and-hold reconstruction, as well as two parametric methods all offer significant improvement over the traditional slotting, direct, and reconstruction estimators. Modifications to the test cases will be discussed with the participants during the conference in preparation for further testing.

1. INTRODUCTION

Despite the relative complexity involved with estimating power spectra from data sampled randomly in time, the development of statistical estimators and computational algorithms for calculating power spectra from laser Doppler anemometer (LDA) data began in the early seventies, when the LDA was still in a stage of infancy. This pioneering work resulted in two estimators, the so-called "slotting technique," described by Mayo et al. (1974), Shay (1976), Scott (1974, 1976), and Gaster and Roberts (1975); and a direct transform presented by Gaster and Roberts (1977). Coincidentally, most of these researchers discontinued their activity in this area shortly after this series of publications. Additionally, the problem of velocity bias, identified by McLaughlin and Tiederman (1973), focused attention on simpler velocity statistics, so that the topic of power spectrum estimation for LDA data was of low priority for the LDA community for roughly a decade.

In the mid to late eighties, a gradual rekindling of interest took place as investigators tried to use the power spectrum as a means to study the small scales of turbulence. Comparative studies such as Srikantiah and Coleman (1985) and Tropea (1986), however, indicated that the early estimators possessed a high degree of variance and a susceptibility to velocity bias. Adrian and Yao (1987) also showed that the age old sample-and-hold reconstruction of LDA data led to a filtered noise effect, which obscures the high frequency portion of the spectrum.

At Veldhoven in 1993, the rekindling of interest quickly turned to heated debate as the modern generation of time and frequency domain processors were shown not to improve the quality of power spectrum estimates. Attention thus returned to algorithmic development. Since then, a number of power spectrum estimators have been proposed, ranging from the modifications of the slotting technique to noise filtering reconstruction schemes and parametric methods, such that a comparative overview is necessary. Such comparative tests were recently attempted by Benedict and Gould (1995), Tummers and Passchier (1996a) and Britz and Antonia (1996), but it has become evident that a single research group can no longer implement and thoroughly test all of the estimators which have been proposed. Furthermore, the most useful standards for comparison and necessary range of testing conditions has not been clear.

With this in mind, the present authors are developing a set of simulated and real benchmark LDA data sets to be used by the authors of power spectrum algorithms in assessing the relative performance of their method. As a first attempt at evaluating the effectiveness of this approach, a large number of authors (>30) were invited to participate in computing power spectra from a wide variety of simulated data sets. Results from 7 of these authors have been received and will be presented below. Note that no authors (with the exception of H. Nobach) were aware of the true underlying spectrum before commencing.

The final purpose of the paper is therefore to establish a standard with which new or improved LDA spectral estimators can be compared in the future. Readers interested in obtaining details of the benchmark test or the data sets are invited to access the data generation program at http://www-nt.e-technik.uni-rostock.de/~nobach/benchm.html.

2. DEFINITIONS AND NOMENCLATURE

To this point we have spoken generally of the power spectrum as the quantity of interest. Here, however, we establish terminology and mathematical definitions of the quantities of interest. Participants were asked to estimate the one-sided, autospectral density function (ASDF) defined as

$$G_{uu}(f) = 4\int_0^\infty C_{uu}(\tau)\cos(2\pi f\tau)d\tau \qquad \text{or}$$

$$G_{uu}(f) = \frac{2}{T}\left|\int_{-\infty}^{\infty} u(t)\exp(i2\pi ft)dt\right|^2 \qquad (1)$$

for the autocorrelation with cosine transform or direct Fourier transform approaches respectively. Here $C_{uu}(\tau)$ is the auto-covariance function (ACF) given by

$$C_{uu}(\tau) = \overline{u(t)u(t+\tau)} = \int_0^\infty G_{uu}(f)\cos(2\pi f\tau)df \qquad (2)$$

where $u(t)$ is the fluctuating velocity, $u(t)=U(t)-\overline{U}$ and τ is the lag-time.

To aid in evaluating results, participants were also asked to provide the autocorrelation coefficient function (ACCF) defined as

$$\rho_{uu}(\tau) = \frac{1}{\overline{u^2}}\int_0^\infty G_{uu}(f)\cos(2\pi f\tau)df \qquad \text{or}$$

$$\rho_{uu}(\tau) = \frac{C_{uu}(\tau)}{C_{uu}(0)} = \frac{\overline{u(t)u(t+\tau)}}{\overline{u^2}} \qquad (3)$$

corresponding to their ASDF estimates. Also, quantities such as the integral time scale, T_u, and the Taylor time scale, λ_u, were used as figures of merit in the analysis. Their definitions are given below.

$$T_u = \int_0^\infty \rho_{uu}(\tau)d\tau = \frac{1}{\overline{u^2}}\int_0^\infty C_{uu}(\tau)d\tau = \frac{G_{uu}(0)}{4\overline{u^2}} \qquad (4)$$

$$\frac{1}{\lambda_u^2} = \frac{-1}{2}\left.\frac{d^2\rho_{uu}(\tau)}{d\tau^2}\right|_{\tau=0} = \frac{2\pi^2}{\overline{u'^2}}\int_0^\infty f^2 G_{uu}(f)df \qquad (5)$$

3. DESCRIPTION OF BENCHMARK DATA SETS

Simulated data sets have been used exclusively for this first round of benchmark testing since, for simulated signals, the true spectrum is known an thus systematic errors (biases) can be evaluated. The techniques used for simulation are well established and tested and are based on a conveyor belt model, as described in detail by Fuchs et al. (1992). With this method, a primary time series of evenly spaced samples with extremely high sample rate is first generated. The desired spectral content is obtained by applying the true spectrum as a filter to a Gaussian distributed random noise sequence.

Particles are numerically seeded randomly in space and convected through the LDA measurement volume with the prescribed velocity series to yield a data set consisting of arrival time and velocity (one component). The data validation rate (DVR), $\dot{N}$, is the particles per second and the mean data density is given by

$$\dot{N}_D = \dot{N}T_u = T_u/\tau_m \qquad (6)$$

where τ_m denotes the mean time between validated bursts, i.e. $1/\dot{N}$.

Ultimately the Nyquist frequency of the primary time series determines the maximum frequency which any algorithm can hope to resolve, and round-off errors in the double precision velocity estimates limit the number of decades in amplitude which can be calculated. It is imperative that the Nyquist frequency of the primary time series be set high enough so as not to artificially limit the performance of the estimators. Results returned by the participants indicate that the resolution of the primary series was unfortunately insufficient for certain cases in these first benchmarking tests, although, in general, it was possible to make a useful comparison. Modifications to the simulated data sets will thus be made before testing continues.

Simulated data are described by number of samples, *N*, and data density, $\dot{N}_D$. They are divided into *groups* (of which there are 3) and *cases* (34 in all). For each case, there are 10 data sets. Participants were asked to provide ASDF estimates for each of the ten data sets as well as the average ASDF and average ACCF. The ASDFs for each case were used to calculate the statistical variance of the participants' spectral estimators.

General Characteristics: $\overline{U}=0$, $\overline{u^2}=1\text{m}^2/\text{s}^2$, $N=250000$

Group S-1 (one case)
Band-limited random noise with Gaussian amplitude distribution and a very steep roll-off at 2000 Hz. This flat spectrum makes filtering effects immediately obvious. (primary series DVR: 10 kHz; Poisson sampled DVR: 1 kHz)

Group S-2 (24 cases)
This group exhibits a Pao-like spectrum, which decreases exponentially (in log coordinates) with increasing frequency, and is given by

$$G_{uu}(f) = \frac{C_1\exp\left[-1.5\alpha\left(f/f_d\right)^{\frac{4}{3}}\right]}{1+\frac{1}{\alpha\pi}\left(\frac{f}{f_d}\right)^{\frac{5}{3}}} \qquad (7)$$

where $\alpha=0.1$. There are 6 basic cases for this group as specified in Table 1. Further cases were then created by adding Gaussian noise, one-dimensional velocity bias, or both.

Table 1 Parameters for Group S-2

Case	f_d (Hz)	C_1 (m^2/s^2)	T_u (s)	DVR (Hz) Prim.	$\dot{N}_D$ Pois.	DVR (Hz) Poisson
2-1	3	0.46	0.115	100	0.5	4.35
2-2	30	0.046	0.0115	1000	0.5	43.5
2-3	300	0.0046	0.00115	10000	0.5	435
2-4	3	0.46	0.115	100	10	87
2-5	30	0.046	0.0115	1000	10	870
2-6	300	0.0046	0.00115	10000	10	8700

Cases S-2-1 to S-2-6
3 different integral time scales at 2 different data densities, no noise or velocity bias.

Cases S-2-7 to S-2-12
Same as Cases S-2-1 to S-2-6 but with added Gaussian noise.

By maintaining a constant $\overline{u^2}$ but changing the integral scale, the signal to noise ratio (SNR) is varied and therefore tests an estimator's ability to resolve multiple decades in the presence of noise

Cases S-2-13 to S-2-18
Same as Cases S-2-1 to S-2-6 but with one-dimensional velocity bias (i.e. correlation between instantaneous velocity and particle rate), no noise

Cases S-2-19 to S-2-24
Same as Cases S-2-1 to S-2-6 but with noise and velocity bias

Group S-3 (9 cases)
The spectrum of this data group exhibits a distinct peak at $f_p = 100$ Hz and is described by

$$G_{uu}(f) = 0.256 \exp_{10}\left\{\begin{array}{l} -\frac{5}{3}m_0\left(\lg\frac{f}{1Hz}\right) - \frac{2}{3}m_0\left(\lg\frac{f}{100\,Hz}\right) \\ +2.004\exp\left[-50\left(\lg\frac{f}{100\,Hz}\right)^2\right] \end{array}\right\} \quad (8)$$

Cases S-3-1 to S-3-3
$\dot{N} > 2\pi f_p$, $\dot{N} \approx f_p$, $\dot{N} \approx f_p/5$ without noise

Cases S-3-4 to S-3-6
As above but with a low noise level

Cases S-3-7 to S-3-9
As above but with a high noise level

4. DESCRIPTION OF PARTICIPANTS' ESTIMATORS

A total number of seven participants submitted results as summarized in Table 2. Before giving further details regarding the algorithm used by each participant, a general classification will be introduced, as represented schematically in Fig.1. Most techniques can be classified into one of the following:

- slotting technique and cosine transform
- direct transform
- reconstruction with equi-distant resampling and FFT

In each of the algorithmic routes, additional steps (shown as dashed boxes) can be found, representing various enhancements made by the participants to these basic algorithms. In the following, the three major algorithmic procedures are introduced, and variations implemented by the participants are highlighted.

Table 2 Summary of participants and methods

Participant	Method	References
Ihalainen et al. I	slotting technique	Mayo et al. (1974)
Ihalainen et al. II	S&H reconstruction	Adrian & Yao (1987)
Ihalainen et al. III	linear reconstruction	Saarenrinne et al. (1997)
Ihalainen et al. IV	DQSE method	Marquadt and Acuff (1983), Saarenrinne et al. (1997)
Nobach I	refined S&H recon. with noise suppression	Nobach et al. (1998)
Nobach II	fuzzy slotting technique	
Nobach III	model parameter est.	Müller et al. (1998)
Rajpal	Lomb Scargle method	Rajpal (1995)
Romano	S&H reconstruction	Adrian & Yao (1987)
Sree	slotting technique	Mayo et al. (1974), Sree (1985)
Tummers & Passchier	slotting technique with local normalization and variable window	Tummers & Passchier (1996a, 1996b)
van Maanen	Parametric	van Maanen & Oldenziel (1998)

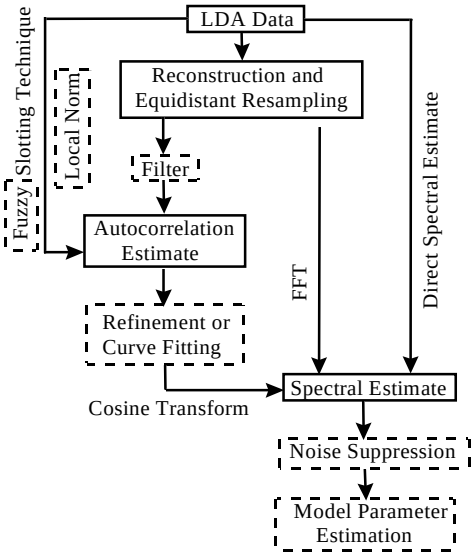

Fig. 1 Schematic for spectrum algorithms

4.1 The Slotting Technique

The slotting technique, generally credited to Mayo et al. (1974), consists of the following algorithm for estimating the discrete autocovariance function,

$$C_{uu}(k\Delta\tau) = \frac{sum\{u_i u_j\}(k\Delta\tau)}{H(k\Delta\tau)} \quad k = 0,1,\ldots,M\text{-}1 \qquad (9)$$

where $sum\{u_i u_j\}(k\Delta\tau)$ represents the sum of all cross products with lag times falling in the time interval (i.e. slot) $(k-0.5)\Delta\tau < (t_j - t_i) < (k+0.5)\Delta\tau$, $H(k\Delta\tau)$ is the number of cross products falling within this slot, and $\Delta\tau$ is the slot width. The parameter M is the number of slots and is chosen by the user.

A one-sided ASDF estimator is formed for the slotting technique by taking its discrete cosine transform as follows.

$$G_{uu}(f) = 4\Delta\tau\left[\frac{1}{2}C_{uu}(0) + \sum_{k=1}^{M-1} C_{uu}(k\Delta\tau)w(k\Delta\tau)\cos(2\pi fk\Delta\tau)\right] \qquad (10)$$

where $w(k\Delta\tau)$ represents a discrete lag window.

Sree. Note that the first slot (k = 0) in the slotting technique is treated separately in Eq. (10) because its width is $\Delta\tau/2$. Normally, the lag products falling within this first slot are ignored (with regard to biases arising from processor dead times and probe volume effects) and the sum of autoproducts is used in place of the sum of cross products. A drawback of using the autoproducts is that they include a noise contribution which biases the autocovariance and ASDF to higher values. Sree thus using only the cross products for the first slot. Otherwise his approach is the standard slotting technique and, referring to the schematic of Fig. 1, follows the path of slotting technique, autocorrelation estimate, cosine transform.

Ihalainen et al. I. The strategy of this group was to include both autoproducts and cross products in the first slot.

Nobach II. A severe limitation of the standard slotting technique is its high variance (roughly constant at high frequency), which leads to poor estimates of turbulence spectra at frequencies well below the mean sampling rate. In order to reduce the variance of the slotting technique, Nobach employs a lag products weighting scheme called the *fuzzy slotting technique* and defined as

$$b_k(\tau) = \begin{cases} 1 - \left|\frac{\tau}{\Delta\tau} - k\right| & \text{for} \quad \left|\frac{\tau}{\Delta\tau} - k\right| < 1 \\ 0 & \text{otherwise} \end{cases} \qquad (11)$$

This scheme allows lag products to contribute to two slots simultaneously and weights lag products that lie close to the slot centers more heavily as seen in Fig. 2.

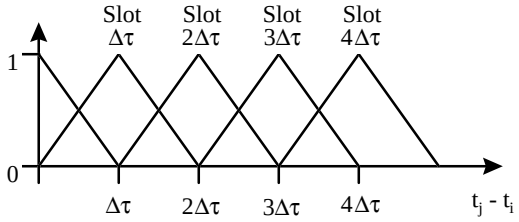

Fig. 2 Fuzzy slotting technique schematic

Tummers & Passchier. Another method for reducing variance in the slotting technique has been dubbed *local normalization* by Tummers and Passchier (1996a, 1996b) and van Maanen and Tummers (1996). In this case, an ACCF normalized by a variance estimate particular to each slot is used as the basis for the cosine transform. This results in the following slotting algorithm

$$\rho_{uu}(k\Delta\tau) = \frac{sum\{u_i u_j\}(k\Delta\tau)}{\sqrt{sum\{u_i^2\}(k\Delta\tau)\,sum\{u_j^2\}(k\Delta\tau)}} \qquad (12)$$

and corresponding one-sided ASDF estimator

$$G_{uu}(f) = 4C_{uu}(0)\Delta\tau\left[\frac{1}{2} + \sum_{k=1}^{M-1}\rho_{uu}(k\Delta\tau)w(k\Delta\tau)\cos(2\pi fk\Delta\tau)\right] \qquad (13)$$

While Eq. 12 has been shown to have significantly lower variance for small lag times than Eq. 9 normalized by $C_{uu}(0)$, the variance at large lag times is unchanged; therefore, the use of local normalization alone does not lead to an improved ASDF. Tummers and Passchier indicate, however, that combining a variable lag window whose lag width decreases with increasing frequency with the local normalization does produce a much improved ASDF.

van Maanen. Here the starting point is also the slotting technique with local normalization, but instead of attacking the variance problem with creative windowing schemes, van Maanen and Oldenziel (1998) recommend curve-fitting the locally normalized ACCF in order to remove variability in the ASDF estimates almost completely. To this end, they have developed an eight-parameter autocorrelation model which is extremely flexible and can be analytically Fourier transformed.

4.2 Direct Transform

Direct transform methods of ASDF estimation are based on the adaptation of the periodogram approach for equispaced data to the case of random sampling. The standard estimator in this regard is that of Gaster and Roberts (1977) given by

$$G_{uu}(f) = \frac{2}{\dot{N}_2^2\,T}\left\{\left|\sum_{j=0}^{N} u'(t_j)d(t_j)\exp(i2\pi ft_j)\right|^2 - \sum_{j=0}^{N} u'^2(t_j)d^2(t_j)\right\} \qquad (14)$$

where $d(t_j)$ is a data window. This estimator has yet to be represented in these benchmarking tests; however, Tummers and Passchier (1996a) have shown that its variability, even

with block averaging, is no better than the slotting algorithm. Benedict and Gould (1995) have also shown that uncorrelated noise results in a negative bias in ASDF estimates using this method. Its advantage is speed in its blockaveraged form.

Rajpal. Scargle (1982) modified the periodogram to make it equivalent to a least squares fitting of sine curves to a data set. His scheme has been applied by Rajpal (1995) and Saarenrinne et al. (1997) to simulated data and turbulent flows.

Ihalainen et al. IV. Another modification to the periodogram is described by Marquardt and Acuff (1983). It this approach, a data spacing factor is incorporated into the periodogram. For Poisson sampling, the factor becomes the inverse of the sampling rate squared.

4.3 Reconstruction with FFT

Reconstruction approaches create equi-spaced time series by resampling according to various interpolation schemes, thereby allowing that an FFT be used in making ASDF estimates. The most common scheme by far is *sample-an-hold* (zero-order). This is the simplest of the polynomial class of reconstruction algorithms.

Adrian and Yao (1987) were the first to call attention to the filter characteristics of reconstruction algorithms. Since then it has been well documented by van Maanen and Tulleken (1994), among others, that the filter effect becomes significant at frequencies under $\dot{N}/2\pi$ in the case of Poisson sampling. If noise is present in the signal, the ASDF estimates can break down well before this filter cut-off. In such a case, additional filtering (see Fig. 1) can be implemented prior to calculating the autocorrelation function. The application of Kalman filtering, for instance, has been investigated by van Maanen and Tulleken (1994) and Benedict and Gould (1995), but has not yet been applied to the benchmarking data.

Ihalainen II and III. implemented the standard sample-and-hold and linear reconstruction schemes respectively.

Romano also implemented the standard sample and hold algorithm.

Nobach I. Recently, Nobach et al. (1998) developed a *refinement* that cancels the filter effect associated with sample-and-hold reconstruction. The approach is to derive an expression for the resampled autocorrelation function in terms of the true autocorrelation function. The relation is then inverted to estimate the true autocorrelation. The ASDF follows from a cosine transform. Referring to Fig. 1, the procedure follows the steps reconstruction, autocorrelation estimate, refinement, spectral estimate. A step for noise suppression can be added when necessary. In principle, a refinement can be derived for any reconstruction algorithm, but it is not always possible to invert the resulting expression.

5 DISCUSSION OF PARTICIPANTS' RESULTS

The flat spectrum (up to a cut-off) data set of Group1 was intended as a prerequisite diagnostic case to ascertain whether a participant's estimator exhibited a filtering effect above a particular cut-off frequency. Only the reconstruction techniques without refinement displayed such filtering. Fig. 3 shows the results for sample-and-hold and linear reconstruction submitted by Ihalainen et al. One may notice that these reconstruction techniques not only filter above a cut-off frequency, but also indicate a positive bias error. This error is reflected in the integral scale errors presented in Table 3 (at the end of the paper). Note that the severity of this bias error is determined by the energy content of the signal at frequencies greater than approximately $\dot{N}/2\pi$. Thus for the spectra presented in Fig. 4, the bias is only significant for the low data rate case. Also note in Fig. 1 that the linear reconstruction has a slightly lower bias error, but that the filter cut-off frequency (visually perceived at $\dot{N}/10$ or 100 Hz) is the same. Thus one should not be fooled by Fig. 4 into thinking that the sample-and-hold scheme has performed better at high data rate than the linear estimator. It is merely coincidence that the sample-and-hold filtering effect better matches the spectrum over this frequency range.

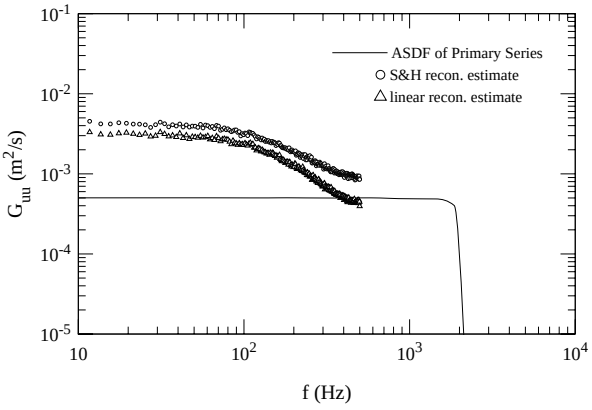

Fig.3 Reconstruction estimators applied to Case S-1

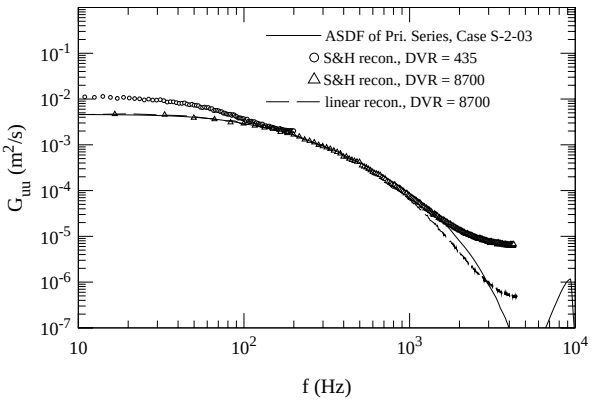

Fig. 4 Results of Romano (low DVR) and Ihalainen et al. for Case S-2-03

Group three was also a set of mainly qualitative diagnostic devices designed to check whether the methods were capable of ascertaining a spectral peak in a wide-band spectrum as various noise levels and data densities. These results require further analysis; however, it appears that all methods

with the exception of the reconstruction methods, which functioned only for the highest data density, were able to determine the peak of 100 Hz. The reconstruction and direct methods were also strongly influenced by noise; although the peak was still recognizable. Finally, the variable window approach of Tummers and Passchier resulted in a significant frequency broadening of the peak, but this was deemed to be a tolerable result.

The Group 2 cases were designed to be indicative of actual turbulence spectra and to allow for some quantitative comparisons of the different methods. It must be admitted that an error in communication between the present authors led to the creation of data sets with relatively low resolution in the primary series. This lessened the value of the comparison to some extent, as a maximum of roughly 5 decades in amplitude could be recovered from the primary time series, but was discovered to late to be corrected in time for the present analysis. Fig. 5 presents a comparison of the true theoretical spectrum and the actual spectrum of the primary time series for Case S2-1. The spectrum of the primary time series is matched well if the exponent in Eq. (7) is considered to be 4.11/3 instead of 4/3.

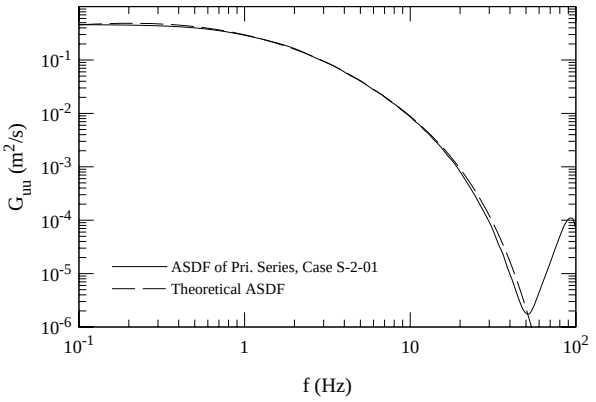

Fig. 5 Comparison of theoretical Group 2 spectra to those obtained from primary time series

Two standards of comparison were estimates of integral scales and microscales, calculated by the present authors from results submitted by the participants (recall that participants were not aware of the exact values during their work). The errors in these time scale estimates are presented in Tables 3 and 4. Some caution should be used in interpreting the microscale results as sometimes biases in different parts of the spectrum canceled in the integration, leading to tolerable microscale estimates. This was the case for the linear reconstruction results of Ihalainen et al. III for example.

Generally speaking, the reconstruction without refinement and direct methods did not perform well for these tests. The reconstruction methods were able to estimate the integral scale only under high data density conditions and the microscale not at all. Noise tended to make both estimates worse. The refinement of Nobach I led to much better results. This is not fully reflected in the table as all the cases for this method have not yet been submitted but are reported to be equivalent to Nobach II. It must be mentioned, however, that the noise suppression scheme employed by Nobach I is not fully convincing. A combination of noise and velocity bias also seems to pose problems.

A surprising result of the comparisons thus far has been the performance of the parametric approaches. The results of Nobach III are excellent in general with problems only occurring for the cases in which velocity bias appears at low data density. The method of van Maanen also appears to be very reliable as the limited results submitted thus far were somewhat unfairly influenced by the resolution of the primary time series. It should be noted that this scheme is designed to most accurately predict the high frequency portion of the spectrum so it is not surprising the integral scale results leave something to be desired. This does not represent a drawback as a better estimate of the integral scale would be available from the locally normalized ACCF when using this method.

As was expected, the standard slotting technique showed a high variance and an inability to cope with noise or bias. Noise problems could be circumvented by using the lag products in the first “half-slot” in place of the autoproducts, however this would rarely be a useful solution under real measurement conditions where processor dead time or the probe transit time limit the minimum inter-arrival time which can be obtained.

The fuzzy slotting technique of Nobach III and the locally normalized slotting technique with variable window implemented by Tummers and Passchier both produced excellent overall results. The method of Tummers and Passchier would appear to be the best of all methods; however, the results presented here can only be considered preliminary. Fig. 6 presents the normalized standard deviation of their ASDF estimates for Case S-2-1 as compared to those of Ihalainen et al. I, achieved with the standard slotting technique at similar frequency resolution. The improvement is obvious.

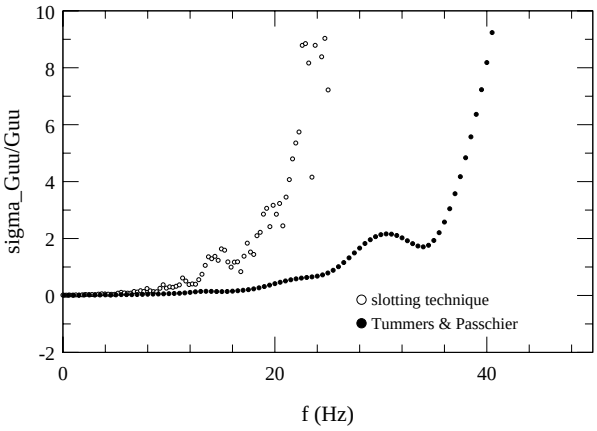

Fig. 6 Comparison of variance of two slotting algorithms

6. CONCLUSIONS

A set of 34 simulated data sets for the testing of power spectrum algorithms for LDA data has been created and made available at the internet address http://www-nt.e-technik.uni-rostock.de/~nobach/benchm.html. Initial results from 7 re-

search groups who have tested 10 algorithms using these data sets have indicated strengths and weaknesses of the algorithms as well as the test cases. Of the algorithms tested, modifications to the slotting technique, known *as local normalization* and the *fuzzy slotting technique* as well as two parametric methods and a refined reconstruction algorithm appear to offer significant advantages over traditional slotting, direct, and reconstruction estimators. Modifications to the test cases will be discussed with the participants during the conference in preparation for further comparative tests. Real LDA data sets will also be considered in the future.

ACKNOWLEDGMENT

The first author wishes to acknowledge the financial support of the Alexander von Humboldt Foundation and National Science Foundation during the course of this work.

REFERENCES

Adrian, R.J. & Yao, C.S. 1987, Power Spectra of Fluid Velocities Measured by Laser Doppler Velocimetry, *Exp. Fluids*, *5*, 17-28.

Benedict, L.H. & Gould, R.D. 1995, Experiences Using Kalman Reconstruction for Enhanced Spectrum Estimates, *ASME/JSME Fluids Eng. and Laser Anem. Conf.,* Hilton Head, SC, Aug. 13-18, FED-Vol. 229, 347-354.

Booij, R. & Bessem, J.M. (Eds.) 1993, Report on Workshop, User's Needs for LDA, Supplement to *Proc. 5th Int. Conf. on Laser Anemometry – Advances and Applications*, Veldhoven, Netherlands, Aug. 23-27.

Britz, D. & Antonia, R.A. 1996, A Comparison of Methods of Computing Power Spectra of LDA Signals, *Meas. Sci. Technol*., *7*, 1042-1053.

Fuchs, W. Albrecht, H. Nobach, H. Tropea, C. & Graham, L.J.W. 1992, Simulation and Experimental Verification of-Statistical Bias in Laser Doppler Anemometry Including Non-Homogeneous Particle Density, *Proc. 6th Int. Symp. on Applications of Laser Techniques to Fluid Mech.*, Lisbon, Portugal, July 20-23, paper 8.2.

Gaster, M. & Roberts, J.B. 1975, Spectral Analysis of Randomly Sampled Signals, *J. Inst. Maths. Applics.*, *15*, 195-216.

Gaster, M. & Roberts, J.B. 1977, The Spectral Analysis of Randomly Sampled Records by a Direct Transform, *Proc. R. Soc. Lond. A.*, *354*, 27-58.

Marquardt, D.W. & Acuff, S.K. 1983, Direct Quadratic Spectrum Estimation with Irregularly Spaced Data, in *Time Series Analysis of Irregularly Observed Data*, ed. Emanuel Parzen, 211-223, Springer Verlag, Berlin.

Mayo, W.T. Jr. Shay, M.T. & Riter, S. 1974, The Development of New Digital Data Processing Techniques for Turbulence Measurements with a Laser Velocimeter, *AEDC-TR-74-53*.

Müller, E. Nobach, H. & Tropea, C. 1998, Model Parameter Estimation from Non-equidistant Sample Data Sets at Low Data Rates, *Meas. Sci. Technol*., *9*, 435-441.

Nobach, H., Müller E. & Tropea, C. 1998, Efficient Estimation of Power Spectral Density from Laser Doppler Anemometer Data, *Exp Fluids*, *24*, 489-498.

Rajpal, A.K.P. 1995, Power Spectrum Estimates of LDA Measurements Using Scargle Perodogram Analysis, *ASME/JSME Fluids Eng. and Laser Anem. Conf.,* Hilton Head, SC, Aug. 13-18, FED-Vol. 229, 411-415.

Saarenrinne, P. Soini, S. Ihalainen, H. & Kaleva, O. 1997, Turbulence Spectral Power Density Estimation for Laser Doppler Anemometer Measurements in a Mixing Tank Flowfield, to *Proc. 7th Int. Conf. on Laser Anemometry – Advances and Applications*, Karlsruhe, Germany, Sept 8-11.

Scott, P.F. 1974, Random Sampling Theory and its Application to Laser Velocimeter Turbulent Spectral Measurements, *Report No. 74CRD216*, Tech, Info Series, General Electric Co., Corporate Res. and Development.

Scott, P.F. 1976, Distortion and Estimation of the Autocorrelation Function and Spectrum of a Randomly Sampled Signal, Ph.D. thesis, Rensselaer Polytechnic Institute, Troy, NY.

Shay, M.T. 1976, Digital Estimation of Autocovariance Functions and Power Spectra from Randomly Sampled Data Using a Lag Product Technique, Ph.D. thesis, Texas A&M University, College Station, TX.

Srikantiah, D.V. & Coleman, H.W. 1985, Turbulence Spectra from Individual Realization Laser Velocimetry Data, *Exp. Fluids*, *3*, 35-44.

Tropea, C. 1986, Turbulence-induced Spectral Bias in Laser Anemometry, *AIAA Journal*, *29*, no. 3, 306-309.

Tummers, M.J. & Passchier, D.M. 1996a, Spectral Analysis of Individual Realization LDA Data, *Report LR 808*, Faculty of Aerospace Engineering, Delft University of Technology, Delft, The Netherlands.

Tummers, M.J. & Passchier, D.M. 1996b, Spectral Estimation Using a Variable Window and the Slotting Technique with Local Normalization, *Meas. Sci. Technol*., *7*, 1541-1546.

van Maanen, H.R.E. & Oldenziel, 1998, Estimation of Turbulence Power Spectra from Randomly Sampled Data by Curve-Fit to the Autocorrelation Function Applied to Laser Doppler Anemometry, *Meas. Sci. Technol*., *9*, 458-467.

van Maanen, H.R.E. & Tulleken, H.J.A.F. 1994, Application of Kalman Reconstruction to Laser-Doppler Anemometry Data for Estimation of Turbulent Velocity Fluctuations, *Proc. 7th Int. Symp. on Applications of Laser Techniques to Fluid Mech.*, Lisbon, Portugal, July 11-14.

Table 3 Integral scale (T_u) errors for Group 2 (in percent)

Case	Iha I	Iha II	Iha III	Iha IV	Noba I	Noba II	Nob III	Rajpal	Roman	Sree	Tumm	Maanen
S2-01	0.49					1.6	1.3		160	-1.0	-7.5	
S2-02	1.7			-74		1.6	1.3		160		-7.5	
S2-03	1.1					1.6	1.3		160		-7.5	
S2-04	2.0				0.57		2.5	-95	1.5		-6.1	
S2-05	-1.0				0.57		2.4	-50	1.5		-6.1	
S2-06	-15	4.0	3.5		0.57		2.4	400	1.5		-6.1	
S2-07	0.44					1.5	1.1		150	-1.1	-7.6	
S2-08	1.7					1.5	1.1		150		-7.6	
S2-09	0.15					1.5	1.1		150		-7.6	
S2-10	1.9				0.64		2.4	-95	-6.4		-6.2	-16
S2-11	-0.66				0.64		2.2		-6.4		-6.2	
S2-12	-15	4.7			-0.64		2.3		-6.4		-6.2	-22
S2-13	270					-0.12	1.5			260	-6.2	
S2-14	260			7.8		-0.12	1.4				-6.2	
S2-15	270					-0.12	1.4				-6.2	
S2-16	260					3.7	2.4				-6.6	
S2-17	260					3.7	2.4				-6.6	
S2-18	270	24	20			3.7	2.5				-6.6	
S2-19	270				160		160		160	260	-0.26	
S2-20	260				160		160		160		-0.26	
S2-21	270				160		160		160		-0.26	
S2-22	260				18		17		-1.4		-1.5	
S2-23	260				18		17		-1.4		-1.5	
S2-24	260				18		17		-1.4		-1.5	

Table 4 Taylor micoscale (λ_u) errors for Group 2 (in percent)

Case	Iha I	Iha II	Iha III	Iha IV	Noba I	Noba II	Nob III	Rajpal	Roman	Sree	Tumm	Maanen
S2-01	-1.7					-16	1.1		-9.1	5.1	-6.3	
S2-02	-1.6			120		-16	1.1		-9.1		-6.3	
S2-03	-16					-16	1.1		-9.1		-6.3	
S2-04	-1.8				-13		-11	-18	-28		-5.5	
S2-05	-2.5				-13		-6.6	-74	-28		-5.5	
S2-06	-10	-28	11		-13		-6.6	-92	-28		-5.5	
S2-07	0.63					8.6	3.1		-9.7	6.4	-4.3	
S2-08	-12					8.6	3.1		-9.7		-4.3	
S2-09	-54					8.6	3.1		-9.7		-4.3	
S2-10	-2.0				27		-5.5	-18	-49		-5.3	-5.4
S2-11	-14				27		-2.7		-49		-5.3	
S2-12	-47	-51			27		-2.7		-49		-5.3	-7.6
S2-13	0.47					-32	-29			-18	-3.9	
S2-14	-----			-14		-32	-26				-3.9	
S2-15	-----					-32	-27				-3.9	
S2-16	-3.0					-1.1	-2.4				-4.6	
S2-17	-----					-1.1	-2.4				-4.6	
S2-18	-----	-31	19			-1.1	-2.4				-4.6	
S2-19	1.9				-52		-38		-4.6	-18	3.4	
S2-20	-----				-52		-28		-4.6		3.4	
S2-21	-----				-52		-36		-4.6		3.4	
S2-22	-5.0				20		6.5		-46		1.5	
S2-23	-----				20		6.5		-46		1.5	
S2-24	-----				20		6.5		-46		1.5	